

548-20
006631
NASA

N89-27755

88-074

ELECTRODE EROSION IN STEADY-STATE ELECTRIC PROPULSION ENGINES*

Thomas J. Pivrotto and W. D. Deininger

Jet Propulsion Laboratory
California Institute of Technology
Pasadena, California

ABSTRACT

The anode and cathode of a 30-kW class arcjet engine have been sectioned and analyzed. This arcjet was operated for a total time of 573 hours at power levels between 25 and 30 kW with ammonia at flow rates of 0.25 and 0.27 gm/s. The accumulated run time was sufficient to clearly establish erosion patterns and their causes. The type of electron emission from various parts of the cathode surface was made clear by Scanning Electron Microscope analysis. A Scanning Electron Microscope was used to study recrystallization on the hot anode surface. These electrodes were made of 2% thoriated tungsten and the surface thorium content and gradient perpendicular to the surfaces was determined by quantitative microprobe analysis. The results of this material analysis on the electrodes and recommendations for improving electrode operational life time are presented.

1. INTRODUCTION

Arcjet thrusters are being developed by both NASA and the Air Force, for space applications, because their high performance allows many important missions to be accomplished with much less propellant than would be required by chemical propulsion systems. The current NASA launch charges are about \$6,000/kgm; hence the use of electric thrusters for orbit change, north-south stationkeeping, attitude control and deep space exploration will result in substantial cost savings. Some communication satellites are already using electric thrusters (resistojets) and the next planned development will be to substitute more efficient arcjets for the resistojets. Some other missions that are seriously considering the use of electric thrusters are the Space-Based-Radar (arcjets), the SP-100 Reference Mission (arcjets), and the Manned-Mars Mission (Magnetoplasmadynamic Arc).

To be effective, these thrusters must operate reliably for very long periods of time; 1000 to 1500 hours per thruster is the current goal. As far as it now is known, the only life-limiting mechanism is electrode erosion. This was shown clearly in a long-duration test of a 30-kW class arcjet run on ammonia.¹ In this test the arcjet ran for a total accumulated run time of 573 hours. During this period both cathode and anode eroded; however, it is believed that the final engine shutdown was due to shorting caused by cathode tip erosion.

These electrodes were sectioned and analyzed in an attempt to gain a deeper understanding of the erosion process as a background for designing an

improved arcjet engine. It is hoped that the results of this analysis will also be useful in the development of magnetoplasmadynamic (MPD) arc thrusters as well.

1.1 Apparatus and Tests

A schematic drawing of the arcjet thruster used in the long-duration test of Reference 1 is shown in Figure 1. The plenum chamber, constrictor and supersonic nozzle were turned from a single piece of 2% thoriated tungsten. The nozzle had a 38° total expansion angle and an exit diameter of 2.41 cm. The constrictor had a diameter of 0.51 cm and a length of 1.07 cm and the plenum chamber had a diameter of 2.03 cm and a 50° half-angle taper at the constrictor end. This nozzle block was fitted into a cylindrical molybdenum body with a 7° taper as shown in Fig. 1. A gas-tight seal was effected between the tungsten and molybdenum by carefully lapping the parts together. High-pressure nitrogen was used to test for and assure a gas-tight seal after assembly of the engine.

The cathode was also made of 2% thoriated tungsten and was 0.95 cm in diameter, 18 cm long and had a 60° included angle tip and a 0.15 cm radius point. The axial gap between the cathode cone and the constrictor entrance was set to 0.21 cm. The cathode was held concentric to the constrictor and plenum chamber with a cylindrical insulator made of high purity (high temperature) boron nitride as shown in Fig. 1. The propellant was injected into the plenum chamber through four 0.15 cm diameter holes drilled through the boron nitride. The downstream ends of these four blind holes were met by four 0.15 cm diameter holes drilled into the end surface of the boron nitride cylinder at an angle of 30° to a line normal to the plane of the figure. In this way the propellant was injected tangentially into the plenum chamber at a radius of 0.75 cm and with a downstream inclination of 30°.

The ammonia propellant was fed into the engine through a stainless steel tube welded into a flange made of Inconel 600 as shown in Fig. 1. The back end of the engine was closed with a 1.91 cm thick disk of boron nitride. All corners of this disk had to be well-rounded to prevent cracking. A standard swaglock bulkhead fitting was used to seal the cathode at the boron nitride disk. A 2.54 cm diameter by 0.25 cm thick stainless steel washer was welded to the fitting, as shown, in order to increase the bearing surface area on the boron nitride. A cylinder of boron nitride with a square, helical groove machined in its outer surface was used to help force most of the incoming propellant to flow along the hot inner surface of the molybdenum body to reduce the heat flow back to the graphite seals. Some propellant also flowed between the boron nitride cylinder and the cathode to help cool the cathode.

*This paper was previously published under the title "Analysis of a Used Pair of Arcjet Electrodes," in Vol. 872 of the SPIE Proceedings, 1988.

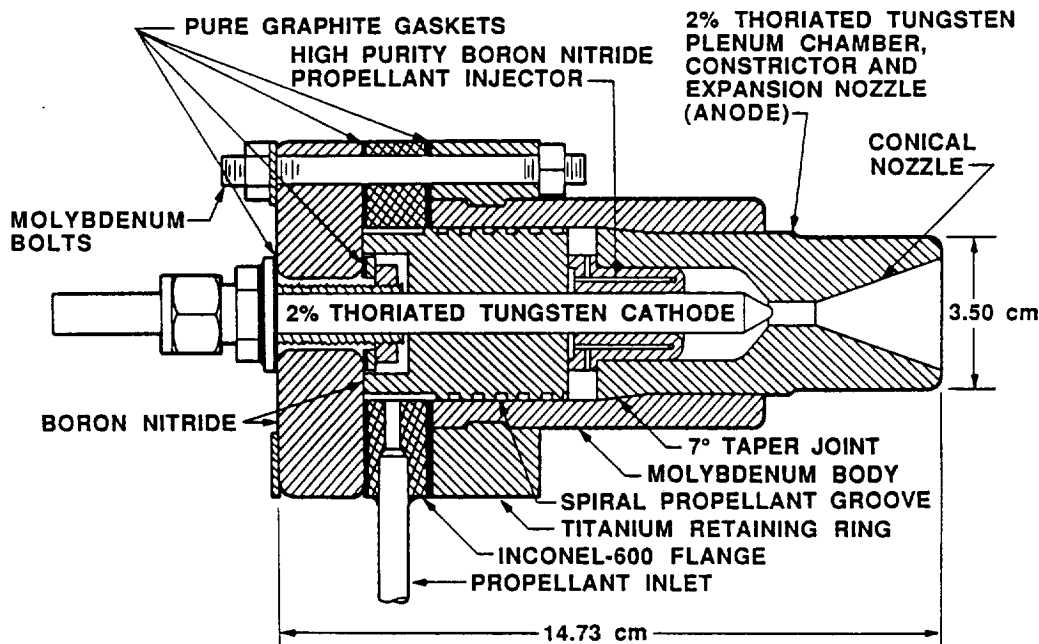


Fig. 1: Schematic of high-temperature Radiation-cooled arcjet engine.

A split ring of titanium was used to engage the molybdenum body through a matching groove machined into the molybdenum as is shown in Fig. 1. The back end of the engine was held together by eight 0.64 cm diameter molybdenum bolts that ran through the boron nitride disk, inconel flange and titanium retaining ring.

Spaces between the swaglock fitting and the boron nitride disk, between the boron nitride disk and the inconel flange and between the flange and the molybdenum body were sealed with 0.08 cm thick pure graphite gaskets. This material is capable of sealing up to a temperature of 3316°C in an inert atmosphere. The eight bolts were torqued to 2.82 N-m and the seals leak checked with high-pressure nitrogen. No leaking was evident. However, after operating the engine at high temperature and then allowing it to cool to room temperature, the torque was found to be greatly decreased. This result indicates that during high-temperature operation the boron nitride, inconel and titanium expand more than the molybdenum bolts, thus further compressing the graphite gaskets, and possibly stretching the bolts and/or nuts.

A complete description of the facility used for long-duration testing of arcjet thrusters can be found in Ref. 2. Briefly, the thruster was mounted on a thrust stand inside a water-cooled stainless steel vacuum tank that was 1.2 meters in diameter and 2.1 meters long. This tank was continuously pumped with a 6.3 m³/s mechanical pumping system and this capacity was sufficient to maintain a vacuum tank pressure of about 70 mtorr when the continuous ammonia mass flow rate was 0.25 gm/s and the arc power was 25 kW. Power for the arc was obtained from a plasma cutting torch power supply capable of providing 400 A at 215 V steady state. The ammonia propellant was guaranteed to be 99.995% pure and was stored in a 1000 kgm tank. The vapor flow rate was controlled and monitored with a commercially available flow controller.

The testing was monitored automatically with a Data Acquisition/Control Unit (DACU) and a desk-top computer. The input data was propellant flow rate,

arcjet current and voltage, thrust stand input and output voltages, vacuum tank and propellant feed system pressures, Radiometer output and various thermocouple signals. The raw data was used to calculate and present arcjet input power, thrust, specific impulse and overall efficiency in real time. The DACU system was also used to monitor the operation, including itself, and was able to shut down the test in an orderly fashion if anything critical was found out of tolerance.

For the first 109 hours the arcjet was operated continuously at a power of 28.6 ± 0.5 kW and an ammonia mass flow rate of 0.25 gms/sec. A facility failure caused a shutdown at that point in time. For the remainder of the test (464 hours) the arcjet was operated at a power of 25.1 ± 1 kW and a mass flow rate of 0.27 gm/s. During the remaining 464 hours of testing the test was interrupted an additional three times because of facility failures. These occurred at 113, 151 and 369 hours into the test. After termination at 573 hours the thruster was disassembled and analyzed.

2. RESULTS AND DISCUSSION

2.1 Cathode

A before and after picture of the cathode tip is shown in Fig. 2. The before picture is actually a second cathode that is identical to the original shape of the test cathode. An oblique view of the test cathode is shown in Fig. 3. Notice that a crater was carved into the cathode tip and a ring of whiskers grew out from the crater rim. The net cathode mass loss over the full 573 hours was 1.95 ± 0.15 gms, for an average loss rate of 3.4 mg/hr. The net volume loss was 0.1 cm³. Notice, from Figure 1, that the whiskers grew toward the anode and that the minimum electrode gap was 1 mm. It is surmised that at 573 hours into the test, one of those whiskers either touched the anode or got close enough to establish a high current arc between it and anode wall. The rush of current, approximately 200 A, through the whisker melted it and surface tension

drew the molten tungsten into a ball on the cathode. Such a ball can be seen in Fig. 3 at about 4 o'clock. The DACU detected a terminal voltage of 99.9V and, since the lower tolerance limit was set at 100.0 V, it terminated the test. Based on this supposition, the controlling of whisker growth and/or providing for it in the thruster design becomes a major goal for achieving a longer operational life time. It has been suggested (Ref. 3) that the growth of cathode whiskers may be influenced by power supply ripple.

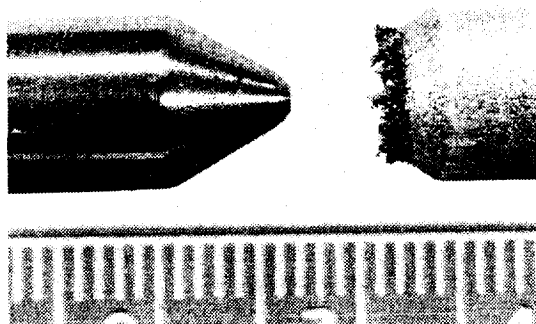


Fig. 2: Picture of cathode tip before and after long duration test.

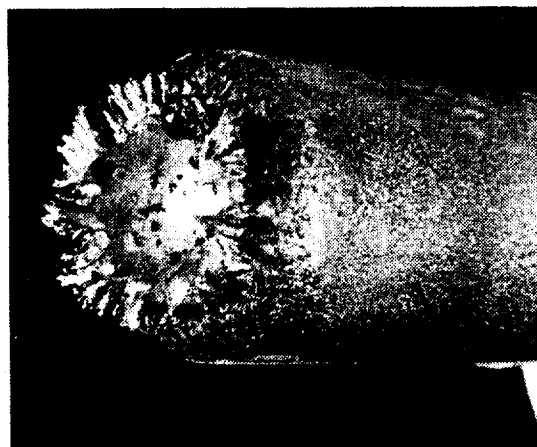


Fig. 3: Close-up picture of cathode tip after long duration test.

The cathode tip was sectioned, polished and etched. A picture of the section is shown in Fig. 4. Notice that the crater has an almost perfect hemispherical shape and that the whiskers are growing radially outward. This type of arcjet cathode cratering has been seen and reported in the literature (see Ref. 4 for example); however, to the best of our knowledge, no one has presented a model or detailed experimental measurements concerning this type of cratering phenomenon, nor has any possible explanation been put forth to date.

One possible cause of this deep, symmetric cratering may have been a jet of gas flowing toward



Fig. 4: Picture of cathode tip cross section.

the cathode tip and centered on the arc centerline. This flow would stagnate on the cathode tip and then flow radially outward over the cathode emitting surface, resulting in the transport of tungsten vapor from the molten emitting surface to the rim of the crater where recrystallization, in the form of whiskers, may have occurred. This concept, shown schematically in Fig. 5, is based on the following considerations. The result of the interaction between the axial arc current and its own azimuthal magnetic field is an inward-directed radial body force. To balance this body force, a radial pressure gradient is set up such that the gas pressure on centerline is higher than the ambient pressure. This pressure difference, $\Delta P(r)$, is taken from Ref. 5 and is given by:

$$\Delta P(r) = \frac{\mu}{4\pi^2} \left(\frac{i}{r_0} \right)^2 \left[1 - \left(\frac{r}{r_0} \right)^2 \right]$$

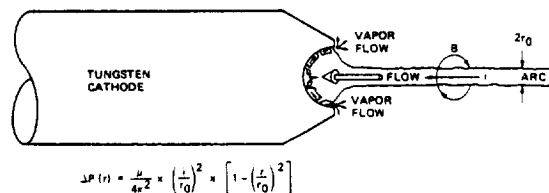


Fig. 5: Proposed cause of cathode tip cratering.

Here, μ is the permeability, i is the total arc current, r_0 the local arc radius and r the radial space variable. The pressure on the arc centerline, relative to ambient, is obtained by setting $r = 0$. The observed arc radius was about 0.75 mm; hence, for a current of 200 A, ΔP was about 18 mm Hg. As is shown in Figure 5, the arc radius must bulge out near the cathode since, due to thermionic emission considerations, the cathode surface area required to feed the arc was much larger (41 mm²) than the 1.8 mm² arc cross-sectional-area. Because of this bulging out, to approximately a radius of 2.5 mm, ΔP , near the cathode surface was reduced to about 2 mm Hg, resulting in an axial pressure gradient of about 32 mm Hg/cm, assuming the ambient pressure was constant. It was this axial gradient that may have driven a flow of very hot gas toward the cathode surface and it then would have convected the tungsten

vapors radially out along the emitting surface, resulting in the deep, symmetric cavity. Additionally, as the arc radius bulges out, an axially directed electromagnetic body force component would have developed, further enhancing the flow of hot gas toward the cathode tip. This additional flow would have turned radially outward along the cathode emitting surface, because of symmetry, and would have added to the convection of tungsten vapor toward the crater rim. These vapors are presumably convected out to the rim of the crater where, apparently, the temperature is low enough to promote epitaxial growth of the whiskers from the tungsten vapor.

Another possible source of tungsten, to feed whisker growth, could have been a tungsten ion current. However, a careful analysis of the rim area with a scanning electron microscope revealed no micro-arc spots or other evidence of current collection.

An experiment is being designed to validate the above concept. This experiment will involve blowing a low-pressure, small diameter jet of hot gas against the locally heated surface of some easily sublimated material, such as camphor, to study crater formation and vapor transport.

As is also shown in Fig. 5, the arc root is connected to the cathode surface through a multitude of dancing micro-arcs since the gas conductivity near the surface is severely limited by the gas temperature which must be in near equilibrium with the surface temperature. The surface temperature can't, on average, be much different from the melting temperature of tungsten (3400°C). Because of the low conductivity the current must be carried across this layer by high current density micro-arcs. Fig. 6 is a head-on view of the cavity and shows that over 90%

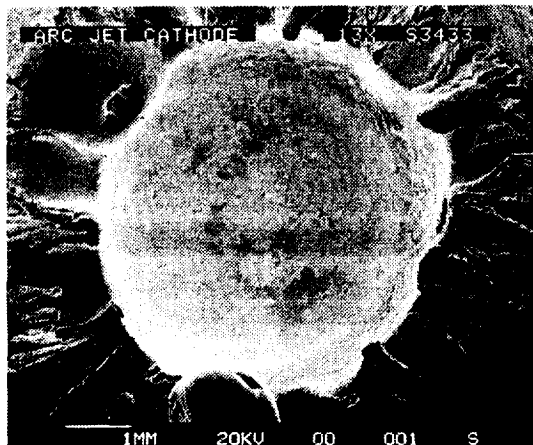


Fig. 6: SEM picture of cathode emission surface.

of the cavity surface is covered with pits caused by the micro-arcs. These individual micro-spots can be more clearly seen in Fig. 7. The spot diameter appears to be about 10 μm and is surrounded by splashed tungsten, clearly indicating the presence of molten tungsten. The reason for these spots dancing over the electrode surface is discussed in Ref. 6. Using data from Ref. 7, at the melting point the tungsten vapor pressure is 17 mtorr, the evaporation rate is $2.28 \times 10^{-4} \text{ gm/cm}^2\text{-sec}$ and the thermionic emission is 479 A/cm^2 . Ignoring the tungsten redeposited as whiskers and taking the total loss as 1.95 gms and the total run time as

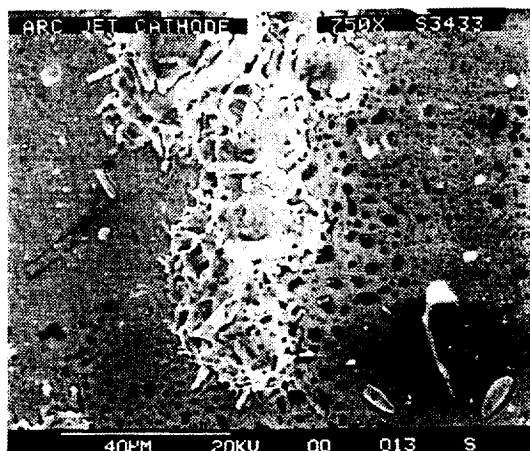


Fig. 7: SEM picture of arc micro spots.

573 hours, we get an average vaporization rate of $9.5 \times 10^{-7} \text{ gm/sec}$. Dividing this by the arc current results in a tungsten loss of $4.3 \times 10^{-3} \mu\text{g/coulomb}$. This result should be compared with the measured loss of $3 \times 10^{-2} \mu\text{g/c}$ and the calculated loss of $10^{-2} \mu\text{g/c}$ found in Ref. 6. The pressure at the cathode tip was probably higher in the current experiment than it was in Ref. 6 and that may be the reason for the reduced loss.

3. ANODE/NOZZLE

The anode/nozzle of a 30-kW class radiation-cooled arcjet must be allowed to operate at elevated temperatures in order to directly dissipate the engine waste heat. This waste heat amounts to about 10% of the total engine power (Ref. 8). An attempt was made to calculate the heat transfer path and resulting isotherms, through the nozzle, in Ref. 8. The results of these calculations are shown in Fig. 8. Note

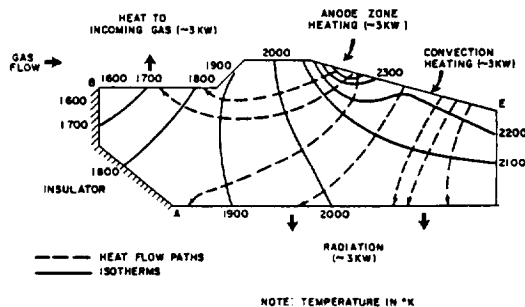


Fig. 8: Results of calculations of heat flow and isotherms in nozzle block.

that the maximum temperature is at the anode arc root and that it can be as high as 2500 K. The rest of the nozzle inner surface is between 2200 and 2300 K and the constrictor is at 2000 K. The outer surface temperature of the arcjet engine shown in Fig. 1 was measured at a point one cm aft of the exit plane with an IR radiometer. The results of this measurement are shown in Fig. 9. The measurement shows a temperature of 2050°C whereas the calculation of Ref. 8 gives 2050°K or 1777°C, a difference which could be because the model used hydrogen as propellant

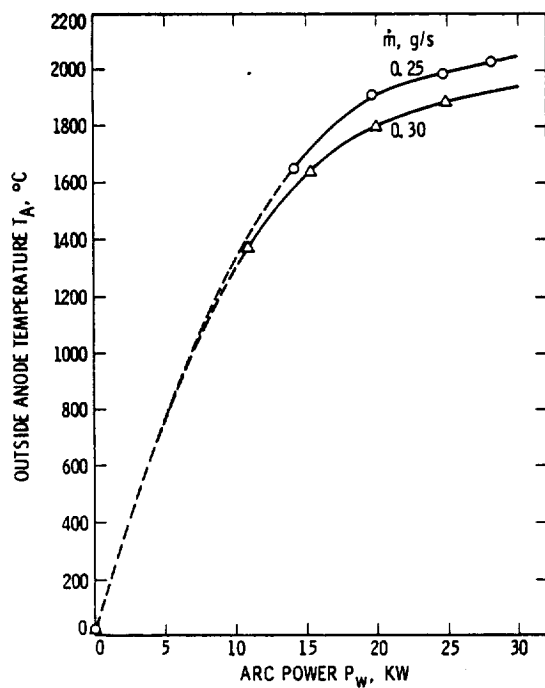


Fig. 9: Effect of arc power and ammonia mass flow rate on outside anode temperature.

and the measurements were made on an ammonia engine, which is known to operate at higher temperatures.

After completion of the long duration test and subsequent attempt at a restart the anode-nozzle was sectioned and the less damaged half was ground flat and smooth. A picture of this half is shown in Fig. 10. The lower contour of the constrictor

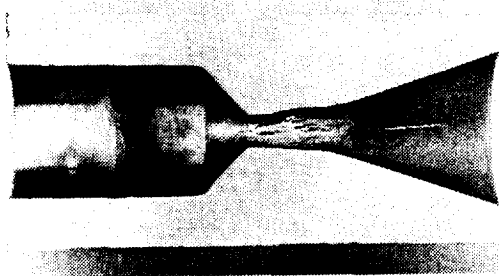


Fig. 10: Sectioned anode block after 573 hours of accumulated run time.

was undamaged and clearly shows the erosion pattern caused by the long duration test. This contour was carefully measured and the results plotted on a large scale and compared with the original pre-test shape. As can be seen in Fig. 10, the erosion starts at about 1 mm into the constrictor. The constrictor radius then starts increasing at an ever-increasing rate for the next 6.5 mm, is then constant at 3.0

mm for the next 4.0 mm and then slowly blends into the 19° half-angle cone. The erosion ends about 4 mm into the expansion nozzle. By performing a graphic integration on the data, the amount of tungsten eroded was determined to be 0.071 cm³ or 1.37 gms. A careful inspection of the nozzle contour part of this plot indicates that the eroded material may have been deposited on the nozzle wall starting about 11 mm from the exit plane. The thickness of this deposited layer increased linearly and reached about 0.2 mm at the exit plane. The volume and mass of this layer was calculated to be 0.075 cm³ and 1.45 g. Note that these determinations are at best an estimate since they involve very small changes in radius, 0.5 mm for the constrictor and 0.2 mm, maximum, for the nozzle. This result suggests that most of the material, evaporated from the constrictor wall, flowed downstream in the laminar boundary layer and redeposited on the cooler downstream wall of the expansion nozzle and also that there is little net mass loss due to normal operation.

By weighing the nozzle before and after the long-duration test, and subsequent damage, a net loss of 2.4 g was found. This loss must have occurred, primarily, when the constrictor was damaged during the attempted restart. This damage can be seen as a pit in the constrictor wall in Fig. 10. Note, in Fig. 10, that the pit appears to start on a crack in the tungsten wall. That pit may have occurred early in the restart, when the nozzle was still relatively cold. Note also that the plenum chamber walls, though stained, were not affected by the long test duration. The machining marks are still visible on the 50° half angle cone wall.

A quantitative microprobe analysis of the sectioned anode-nozzle was also performed. Ten points were selected along the inner edge of the 50° cone, constrictor and expansion nozzle with a point spacing of approximately 5 mm. A reference point was taken at the very back of the anode nozzle piece. The reference point indicated a thorium content of 1.88 atomic percent with a statistical error of 5.49 percent. Interestingly, about 2 percent molybdenum was also found at this point. Apparently the molybdenum diffused into the tungsten from the engine body during the long duration test. For the rest of the data, the thorium content was 1.2 atomic percent + 0.2 - 0.4 and this data had a statistical error of 6.4% + 2.8 - 1.0. Therefore, a significant amount of thorium was still found in the anode/nozzle surface material. A low concentration of 0.85 atomic percent was found about 5 mm downstream of the end of the constrictor and this is about where the arc is expected to attach to the nozzle, causing increased heating.

These results suggest that the anode/nozzle suffered no damage that was directly due to the arc during normal operation. However, due to the high operating temperatures, most of the constrictor wall and the sharp corner between constrictor and expansion nozzle did evaporate at the rate of approximately 6.6×10^{-7} g/s or 3.0×10^{-3} μg/c. Also, using a Scanning Electron Microscope, the walls of the nozzle where the arc was expected to terminate was studied. No unusual effects could be seen except for a greater depletion of thorium from the area.

4. CONCLUSIONS

4.1 Cathode

It is believed that the engine malfunction at 573 hours into the test was caused by the growth of whiskers on the cathode tip. It is further believed that these whiskers grew from tungsten vapor created inside the hemispherical crater and convected out

to the rim by a slow fluid flow that was pumped by an electromagnetic induced fluid pressure gradient. To alleviate this problem, it may help to machine a cavity into the cathode tip in order to reduce the amount of vapor available for whisker growth. It has also been suggested that the growth of whiskers may be influenced by ripple in the arc voltage/current. If so, a ripple-free power supply may be what is needed.

4.2 Anode/Nozzle

The downstream portion of the constrictor was eroded, probably by evaporation at high temperature. This area of the anode could be better cooled by increasing the radiating surface emissivity, by regeneratively cooling and/or by applying heat pipes to this area.

5. ACKNOWLEDGEMENTS

The research described in this paper was carried out by the Jet Propulsion Laboratory, California Institute of Technology, and was sponsored by the Strategic Defense Initiative Organization, Innovative Science and Technology Office, and the National Aeronautics and Space Administration. The work was performed as part of JPL's Center for Space Microelectronics Technology.

6. REFERENCES

1. T. J. Pivrotto, D. Q. King, J. R. Brophy and W. D. Deininger, "Performance and Long-Duration Test of a 30-kW Thermal Arcjet Engine," Final Report for the Period 28 December 1984 to 30 November 1986, Air Force Astronautics Laboratory, Air Force Space Technology Center, Space Division, Air Force Systems Command, AFAL-TR-87-010.

2. T. J. Pivrotto, D. Q. King and J. R. Brophy, "Development and Life-Testing of 10-kW Class Thermal Arcjet Engines," Presented at the AIAA/DGLR/JSASS 19th International Electric Propulsion Conference, September 30 - October 2, 1985 in Alexandria, Virginia, AIAA-85-2031.

3. Private Communication from Mr. Joseph Cassidy of the Rocket Research Company, Redmond, Washington and Mr. Roger Meyer of the Department of Mechanical and Aerospace Engineering, Princeton University.

4. R. R. John, J. F. Connors and Stewart Bennett, "Thirty Day Endurance Test of a 30-kW Arcjet Engine," AIAA Summer Meeting, Los Angeles, California, paper No. 63-274, 17 - 20 June 1963, and James P. Todd, "30-kW Arcjet Thruster Research," prepared under Contract No. AF33(657)-10338 by Giannini Scientific Corporation, Santa Ana, California for Air Force Aero Propulsion Laboratory, Research and Technology Division, Air Force Systems Command, Wright-Patterson Air Force Base, Ohio, Project No. 3141, Task No. 314101, Technical Documentary Report No. APL-TDR-64-58, March 1964.

5. Robert G. Jahn, "Physics of Electric Propulsion," McGraw-Hill Book Company, 1968.

6. H. O. Schrade, M. Auweter-Kurtz and H. L. Kurtz, "Cathode Erosion Studies on MPD Thrusters," AIAA Journal, Vol. 25, No. 8, August 1987.

7. Handbook of Chemistry and Physics, 51st Edition, 1970 - 1971, The Chemical Rubber Company.

8. Thirty Kilowatt Plasmajet Rocket-Engine Development/Second Year Development Program; Second Quarterly Progress Report, 15 August through 15 November 1962, Prepared by Research and Advanced Development Division, Avco Corporation, Wilmington, Massachusetts for National Aeronautics and Space Administration, Lewis Research Center, Cleveland, Ohio, X64-10449, RAD SR-62-255, Contract Number NAS-5-600, 21 December 1962.